

Study on the Crystallography of the Nd-Ce-Cu-O compounds

Jung-Sik Kim and Kwang Soo Yoo

Dept. of Materials Engineering, Seoul City University, Seoul, 130-743 Korea.

1. Introduction

Two years latter on the discovery of a high-Tc superconductor in the La-Sr-Cu-O system, Tokura et al.[1] discovered a new class of superconductors, $\text{Nd}_{2-x}\text{Ce}_x\text{CuO}_{4-\delta}$, which are n-type superconductors at 24K. The T' $\text{Nd}_{2-x}\text{Ce}_x\text{CuO}_{4-\delta}$ structure has attracted attention for a number of reasons: firstly, it was reported to have electrons rather than holes as the charge carriers in contrast with all previously reported cuprate superconductors and secondly, both cation substitution of Nd^{3+} by Ce^{4+} and a small degree of oxygen reduction are essential for superconductivity. Measurement of the Hall and Seebeck coefficients[2] indicated that the major charge carriers are electrons, while holes are charge carriers in other p-type superconductors. Structurally, rare earth cuprate of $\text{Nd}_{2-x}\text{Ce}_x\text{CuO}_{4-\delta}$ has T' structure in which copper is in four-fold coordination, rather than being in six-fold coordination with four of the oxygen atoms in the CuO_2 plane; hence, electrons can be doped into the CuO_2 sheet. So far, much experimental data[3-8] has indicated that the material-specific microstructural phenomena of the T' $\text{Nd}_{2-x}\text{Ce}_x\text{CuO}_{4-\delta}$ structure may be quite complex.

An intersecting set of higher-order Laue zone(HOLZ) deficiency lines is often visible in the central bright field disc of a convergent beam electron diffraction (CBED). The position of these lines depends sensitively on small variation of lattice parameter, local strain, microscope voltage or composition and can also be affected by dynamical interactions between HOLZ lines. Taking an orientation where dynamical interactions between HOLZ lines are weak, it is possible to determine the microscope voltage and the lattice parameter with high accuracy by matching the experimental CBED patterns with those simulated using a plotting program which is based on the kinematic or plane-wave approximation. The applications of such a program are now frequently appeared as a valuable method to study microstructural defects or other crystallographic characterization.

In the present study, the possible structural change of orthorhombic to tetragonal phase transition accompanying the substitution of Ce and reduction of oxygen in $\text{Nd}_{2-x}\text{Ce}_x\text{CuO}_{4-\delta}$ system were of interest by observing the CBED patterns. Since the positions of higher-order Laue zone (HOLZ) deficiency lines depend sensitively on, among various parameters, small changes in lattice parameter and microscope voltage, it is possible to study the lattice parameter changes accompanying by structural change in cases of the substitution of Ce and the oxygen reduction. Detailed review and study have been done elsewhere [9-10] for the lattice parameter measurement by CBED.

2. Experimental procedure

$\text{Nd}_{2-x}\text{Ce}_x\text{CuO}_{4-\delta}$ polycrystalline samples were prepared by heating in air the mixture of appropriate molar quantities of Nd_2O_3 , CeO_2 and CuO . The mixed powder was ground and pressed to form a pellet, then sintered 3~4 times at intermediate temperatures for 48 hrs prior to the final sintering temperature of 1080 °C at which sample was held for 48 hrs before being quenched to room temperature. In order to

make a sample being a superconductor with reduction of oxygen, it was annealed at 950 °C for 20 hrs in flowing gas of N₂-O₂ mixture which showed the oxygen partial pressure of $p_{O_2} = 10^{-4}$ atm by the YSZ (Yttria Stabilized Zirconia) oxygen sensor. The oxygen content of the reduced sample at the above condition was measured as $4-\delta = 3.965$ in Nd_{1.85}Ce_{0.15}CuO_{4- δ} by thermogravimetric analysis. A resistivity measurement of Nd_{1.85}Ce_{0.15}CuO_{3.965} was performed by the standard four-probe technique and showed the onset point for superconductivity (T_c) at 22.0K and the zero resistance critical temperature (T_{c0}) at 19.6 K.

Samples for the TEM observations were prepared either by Ar-ion milling of dimpled thin discs in a liquid-nitrogen-cooled sample stage or by crushing and suspending powder on a carbon grid. The samples were examined in an electron microscope immediately after the ion milling to minimize any contamination from exposed atmosphere. A JEOL 2000FX transmission electron microscope was used to obtain the convergent beam electron diffraction pattern in a liquid-nitrogen-cooled sample holder, using 200 kV accelerating voltage.

3. Results and discussion

Detailed studies of the possible structural transition were carried out by observing CBED patterns for the Ce-undoped, the Ce-doped/oxidized, and the Ce-doped/reduced samples by CBED patterns. The positions of HOLZ lines in the bright field disc of CBED pattern were compared for the three different samples at several zone axes. The stereographic projection of the tetragonal Nd₂CuO₄ crystal is shown with the Kikuchi maps in Fig.1. The CBED patterns of zone axes such as $\langle 221 \rangle$, $\langle 331 \rangle$ and $\langle 661 \rangle$ between $\langle 001 \rangle$ and $\langle 110 \rangle$ poles were relatively clearer than the other zone axes. Fig.2-4 shows $\langle 331 \rangle$ zone axis patterns for three different samples of Nd₂CuO₄ (Ce-undoped), Nd_{1.85}Ce_{0.15}CuO₄ (oxidized) and Nd_{1.85}Ce_{0.15}CuO_{3.965} (reduced). Comparing the positions of HOLZ lines of the Ce-undoped specimen (Fig.2) with those of the Ce-doped specimen (Fig.3), there are no symmetry break of m_1 . Probably due to the close atomic radius of Nd and Ce ($r_{Nd} = 0.182$ nm, $r_{Ce} = 0.182$ nm), doping Ce⁴⁺ into Nd³⁺ ionic site does not create any orthorhombic distortion from the tetragonal matrix. Also, the comparison of positions of HOLZ lines for the reduced/Ce-doped specimen of $4-\delta = 3.965$ in Nd_{2-x}Ce_xCuO_{4- δ} (Fig.4) with those for the oxidized specimen of $4-\delta = 4.0$ in Nd_{2-x}Ce_xCuO_{4- δ} (Fig.3) shows no symmetry distortion, which indicates that the superconducting phase has the same tetragonal structure of a non-superconducting phase.

Fig.5 shows the CBED pattern of [001] zone axis taken at long camera distance and at the operating voltage of 201.0 kV for Nd_{1.85}Ce_{0.15}CuO₄ specimen. The first-order Laue-zone (FOLZ) ring pattern shows exactly the 4mm symmetry. That is, mirror symmetries in the (100), (010), (110) and (1 $\bar{1}$ 0) planes form a 4-fold axis of rotation along the c-direction. Also, [100] zone-axis CBED pattern showed the FOLZ ring pattern which has a symmetry 2mm of (010) and (001) mirror planes, thus a 2-fold rotation axis in the a-direction. From these results, the Nd_{1.85}Ce_{0.15}CuO₄ compound can be concluded to be a point group of 4/mmm.

The apparent lattice parameter was determined by matching the observed CBED pattern with the computer generated pattern which is based on the kinematic assumption. For the determination of absolute lattice parameter, the microscope voltage should first be measured using, for example, HOLZ lines from weak axes in materials of well-known lattice parameter. In the present study the operating voltage

of electron microscope was measured by fitting the HOLZ lines in the bright-field disc of convergent beam patterns for Si [113] zone axis known as weak axes[11] to computer-generated patterns. Fig.6 shows the CBED pattern of Si [113] zone axis and the operating voltage was determined as 201.0 ± 0.1 kV. The experimental CBED pattern of [331] zone axis was fitted to the computer generated pattern. With known voltage, the lattice parameters of a_0 and c and the positions of cations of Nd and Cu were assumed as unknown variables to fit the observed CBED patterns with the computer-generated ones. In this way the determined lattice parameters of a_0 and c for Nd_2CuO_4 oxide were 0.394 nm and 1.217 nm, respectively with the operating voltage of 201.0 kV.

4. Conclusions

According to the study on the relative intersections of HOLZ lines for samples of Nd_2CuO_4 , $\text{Nd}_{1.85}\text{Ce}_{0.15}\text{CuO}_4$ and $\text{Nd}_{1.85}\text{Ce}_{0.15}\text{CuO}_{3.965}$, any phase separation or structural transition by Ce doping and oxygen reduction conducted to be a superconductor were not taken placed. Therefore, no orthorhombic-tetragonal phase transition which is often present in other cuprate superconducting systems, are appeared in the $\text{Nd}_{2-x}\text{Ce}_x\text{CuO}_{4-\delta}$ superconductor. By matching experimental HOLZ patterns with those computer-simulated using a plotting program the determined lattice parameters of a_0 and c for Nd_2CuO_4 were 0.394 nm and 1.217 nm, respectively.

References

- [1] Y. Tokura, H. Takagi and S. Uchida, *Nature* 337, (1989), 345.
- [2] H. Takagi, S. Uchida and Y. Tokura, *Phys. Rev. Lett.* 62, (1989), 1197.
- [3] J. M. Tranquadan, S. M. Heald, A. R. Moodenbaugh, G. Liang, and M. Craft, *Nature* 337, (1989) 720.
- [4] A. C. W. P. James, S. M. Zahurak and D. W. Murphy, *Nature* 338, (1989), 240.
- [5] J. S. Kim and D. R. Gaskell, *Physica C* 209, (1993) 381.
- [6] R. J. Cava, H. Takagi, R. M. Fleming, J. J. Krajewski, W. F. Peck Jr., P. Bordet, M. Marezio, B. Battlogg, and L. W. Rupp Jr., *Physica C* 199 (1992), 65.
- [7] P. Lightfoot, D. R. Richards, B. Dabrowski, D. G. Hinks, S. Pei, D. T. Marx, A. W. Mitchell, Y. Zheng and J. D. Jorgensen, *Physica C* 168 (1990), 627.
- [8] P. A. van Aken, W. F. Müller and J. Choisnet, *Physica C* 211, (1993), 421.
- [9] J. W. Steeds, *Convergent-beam electron diffraction*, in: *Intr. to Analyt. Elec. Micro.* eds. J. J. Hren, J. I. Goldstein and D. C. Joy (Plenum, NY, 1979), 387.
- [10] Y. P. Lin, A. R. Preston and R. Vincent, in: *Electron Microscopy and Analysis 1987*, Inst. Phys. Conf. Ser. 90, eds. L. M. Brown (Inst. Phys. London-Bristol, 1987), 115.
- [11] Y. P. Lin, D. M. Bird and R. Vincent, *Ultramicroscopy* 27 (1989), 233.

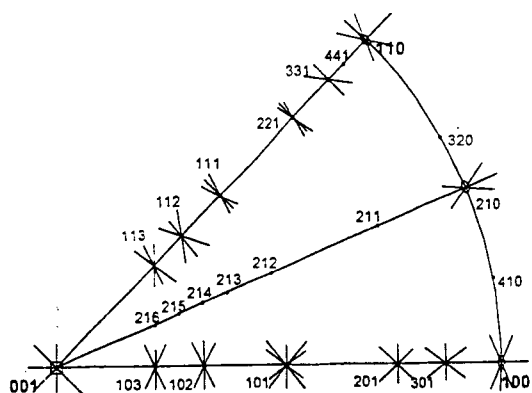


Fig.1. Stereographic projection of the tetragonal crystal, Nd_2CuO_4 .



Fig.2. CBED pattern of $[331]$ zone axis for Nd_2CuO_4 .



Fig.3. CBED pattern of $[331]$ zone axis for $\text{Nd}_{1.85}\text{Ce}_{0.15}\text{CuO}_4$.



Fig.4. CBED pattern of $[331]$ zone axis for $\text{Nd}_{1.85}\text{Ce}_{0.15}\text{Cu}_{3.965}$.

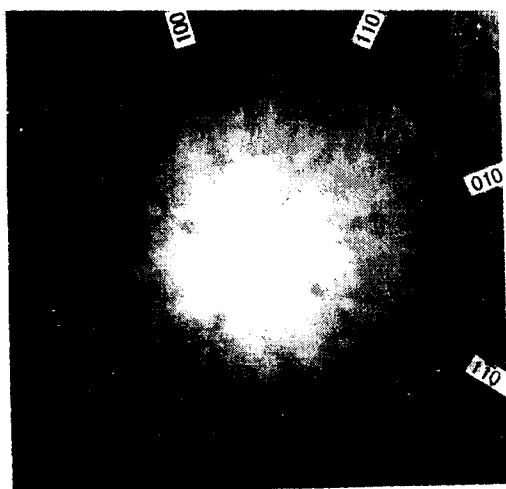


Fig.5. CBED pattern of $[001]$ zone-axis for $\text{Nd}_{1.85}\text{Ce}_{0.15}\text{CuO}_4$.

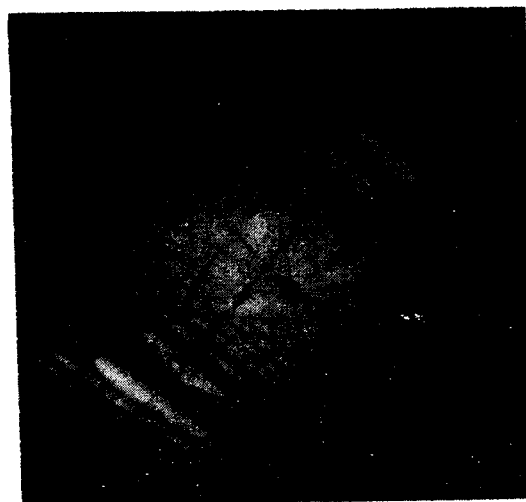


Fig.6. CBED pattern of $[113]$ zone-axis for Si.